

Instrumental Methods of Analysis

Sixth Edition

HOBART H. WILLARD

University of Michigan

LYNNE L. MERRITT, JR.

Indiana University

JOHN A. DEAN

University of Tennessee at Knoxville

FRANK A. SETTLE, JR.

Virginia Military Institute

Wadsworth Publishing Company
Belmont, California
A Division of Wadsworth, Inc.

Hobart H.
urses in in-
orely miss

Settle is
y the elec-
e sections.
ectronics:
Modifying
nents and

st edition
ded from
aphy, gas
and high-

the Sixth
hat most
s or their
methods.
dary ion
and elec-
analysis

chapter
e signals
nd prin-

ew con-
pter on
are not
imetry
id cou-
uch ir

rieve z
hat the
vels o:

CHAPTER 13

Chemical Analysis of Surfaces

Most chapters in this book describe specific methods and their applications to many substances or use in many situations. Due to the recent interest in analysis of surfaces, this chapter will, in a sense, reverse the above procedure and describe several different methods of analyses applicable to qualitative and semiquantitative analyses of surfaces as an aid in surface characterization.

A surface is, theoretically, an infinitely thin layer separating two phases. The scanning electron microscope provides pictures of surface topography at a resolution of about 10 nm. Most analyses are concerned with the interface between a solid and a gas (usually air). Furthermore, in practice the layer of interest has a finite thickness, at least the thickness of an atom or a molecule. One might be interested in determining what is present in the surface layer and whether the surface layer is homogeneous in a direction parallel to the surface. Sometimes, however, there is a concentration gradient in a direction perpendicular to the surface that may extend from atomic dimensions to 10 nm or more. Surface analysis then might involve studying the differences in concentrations of elements at the surface and into the bulk layer by layer. On most technological surfaces the greatest surface compositional changes occur in approximately the first 20 monolayers.

Surface Spectroscopy

Surface spectroscopy involves probing a sample target with a flux of energetic particles and detecting characteristic particles emitted from the surface after interaction. The probe beam may be photons, electrons, or ions.

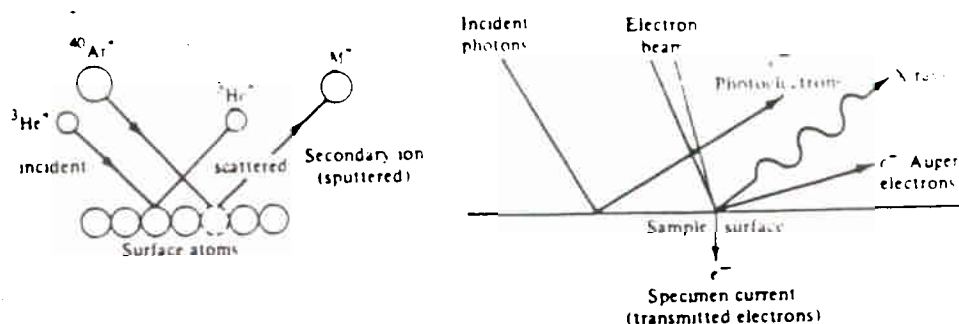


FIGURE 13-1 Energy interchange involved in surface analysis methods.

Surface analysis has many applications, for example, adsorption of contaminants on a surface, adsorption of reacting or interfering molecules on the surface of a catalyst, and segregation of components of the bulk material at a surface or at grain boundaries or imperfections. Corrosion products are identified at the surface where the corrosion is occurring. For conductors, semiconductors, and insulators, one can detect and identify impurities that critically affect bond integrity and the electrical properties. Evaluation of predeposition and cleaning is facilitated. Adhesion studies benefit from the determination of the composition of surface layers that influence adhesive properties of materials. Embrittlement of metals and alloys can be studied in conjunction with in-position fracture of specimens to detect and identify grain boundary impurities that cause embrittlement. Thin film composition can be correlated to electrical, transport, and emission characteristics of the film.

The energy exchange interactions that give rise to these signals may be effectively stimulated by a variety of energy sources (Fig. 13-1). Activation may be by electromagnetic radiation, as in electron spectroscopy for chemical analysis (ESCA), by a beam of incident ions, as in secondary ion mass spectrometry (SIMS) and ion scattering spectroscopy (ISS), or by an incident electron beam as in Auger electron spectroscopy (AES) or electron microprobe (X-ray fluorescence) analysis (discussed in Chapter 9).

Photons of high energy penetrate deeply into a solid; an X-ray beam of 1000 eV may penetrate up to 1000 nm. By contrast, low-energy electrons and low-energy ions have very short penetration depths on the order of 1–2 nm. However, when the ion energy is increased from 10^3 to 10^7 eV, the penetration depth increases from 2.0 to 10^4 nm. A comparison of relative depths of penetration and of analysis volumes for the several surface analysis methods to be discussed in this chapter are shown in Fig. 13-2. Thus, if one wishes to do surface spectroscopy, one should use either low-energy electrons or low-energy ions to limit the sampling depth to roughly 2.0 nm or less.

There are advantages and disadvantages offered by the various sources of incident energy. Excitation by electromagnetic radiation generally provides excellent chemical information but offers poor elemental sensitivity and spatial resolution. Electromagnetic radiation offers the additional advantage of being the least destructive to organic and other highly sensitive surfaces. The use of an incident ion beam generally provides the best elemental sensitivity, but it is limited in spatial resolution. It offers little chemical information and

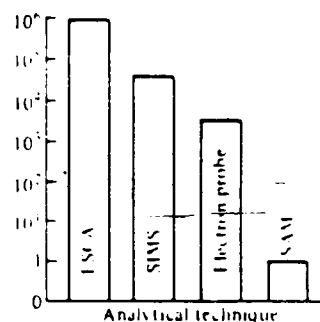
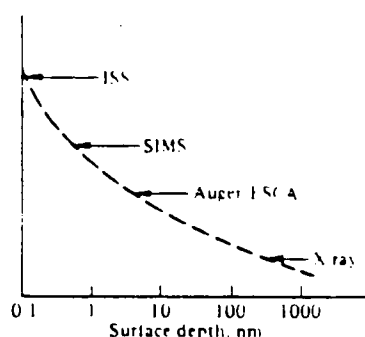
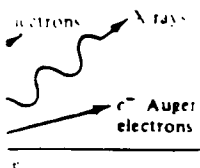


FIGURE 13-2 (a) Comparison of relative depths from which information originates for various surface analysis techniques, and (b) comparison of analysis volumes normalized to scanning Auger microprobe.

it can be used for destructive testing only. The electron beam, on the other hand, offers excellent spatial resolution for sample imaging and analysis. It offers a sensitivity much better than electromagnetic radiation-based techniques and it can be used for nondestructive analysis.

Solids are most conveniently handled as flat pieces. Pulverized material may be pressed into a disk, spread onto a metallic backing, such as abraded aluminum plate, or dusted onto conducting tape. Liquids may be handled if frozen on a cryostat finger.

Problems Unique to Surface Analysis

Samples must be transferred from their point of origin to the spectrometer without contacting air, which may alter the surface, giving erroneous results. This would be particularly critical when examining an active catalyst.

For most solid surfaces, adsorption of residual gases in a vacuum chamber occurs at an approximate rate of 1 monolayer/sec at 10^{-6} torr. A vacuum of 10^{-10} torr provides analysis times on the order of 30 min before about one-tenth of a monolayer of residual gas (more than enough to contaminate the surface) is adsorbed. In vacuums of only 10^{-5} to 10^{-6} torr, heavy contamination from pump oil is a problem. All the techniques to be discussed in this chapter have a shallow escape depth for the analytical signal and consequently place the most stringent requirements on the cleanliness of the residual vacuum in the vicinity of the sample surface. The presence of a surface contaminant will attenuate the analytical signal coming from the true sample and add the contaminant's characteristic spectrum to that of the real sample.

An even more severe problem is the possible disruption of a surface by the measurement techniques themselves. Little surface disruption occurs in ESCA and the measurements are characteristic of the surface. Charging effects can be compensated. AES is more destructive and is particularly bad for organic materials. Electrons are chemically active and thus can cause chemical effects. These effects will usually be most severe in insulators and least in conductors. Again the charging effect can be compensated. SIMS and ISS, tech-

niques that use sputtering as the mechanism of obtaining surface information, will disrupt the surface. However, in the static SIMS mode the beam current density incident on the surface is kept at a low level, which corresponds to removal of about one monolayer in 10 hr. Thus, although SIMS causes long-term disruption, particularly in dynamic SIMS, short-term information (15 min) can be characteristic of the intact surface layer. Dynamic SIMS uses larger beam currents and does not attempt to preserve the outer layer of a surface. In fact, dynamic SIMS experiments scramble about 2.0–5.0 nm of the surface and, at best, give analyses averaged over several atomic layers.

Distribution of Surface Species

The composition of surfaces is not necessarily the same as the bulk. Frequently, in otherwise homogeneous solid systems, inhomogeneities occur as one approaches an interface. The distribution of surface species becomes an important parameter when considering chemical analysis of a surface. Surface analysis that is independent of the instrumental technique occurs only if the information depth of the technique is small relative to the concentration profile. A combination of the nature of the distribution of species and the actual measurement depth used can create vastly different ratios of measured components.

If the interaction volume being probed in a particular measurement is homogeneous and consists of a single surface phase, it can be straightforward to deduce elemental concentrations from the observed intensities. Real samples, however, can be expected to be inhomogeneous and it is a demanding task for the analyst to ensure that meaningful measurements are made.

Sputter-Etching, Depth Profiling, and Elemental Imaging or Mapping

The procedures used to obtain clean specimens include argon ion sputtering, scribing, and bake-out. The high vapor pressure of many reactive metals may prevent attainment of ultra-high vacuum through bake-out. Most spectra are obtained during argon ion sputtering. This technique produces relatively clean surfaces without baking the system. A sputtering rate of about 1.0 nm/min is considerably faster than the adsorption rate of active residual gases.

For many highly reactive metals the surface oxide layer may be too thick for convenient removal by sputtering. A more expedient method for producing a clean surface is to scribe the surface with a carbide tip. The base of the scratched groove should be about as wide as the probe beam diameter.

Depth profiling analysis can be done in conjunction with a noble gas ion beam for sputtering etching of a surface. This technique extends the spatial resolution provided in the plane of a surface to the depth dimension. The process involves bombardment of the specimen surface with a beam of argon or xenon ions to sputter etch the specimen surface while simultaneously bombarding the specimen with the electron beam (for AES) or with an X-ray beam (for ESCA). It is important that the sputter-etched area be much larger than the area of the electron or photon beams so that the region of analysis is in the center of a relatively flat-bottomed crater. This precludes analysis of the sides of the crater, where

formation, will disrupt density incident on the out one monolayer in only in dynamic SIMS, surface layer. Dynamic e outer layer of a sur- of the surface and,

the depth resolution would be seriously impaired. In typical equipment the ion beam diameter is of the order of a few millimeters, while the electron or photon beam might be focused down to 25 μm . Typical etching rates are variable up to about 3.0 nm/min.

Raster/gating permits automatic scanning of the probe beam over a preselected surface area. The gating circuit can be used in conjunction with the rastering beam to restrict data collection to a smaller area than the scanned beam is covering. Elemental analysis can be secured by simply scanning across the specimen or by focusing on selected points.

13.1 ION SCATTERING SPECTROMETRY (ISS)

bulk. Frequently, in approaches an inter- meter when consider- of the instrumental small relative to the on of species and the easured components. ment is homogeneous educe elemental con- can be expected to be that meaningful mea-

ISS involves observing a binary elastic collision between an incident noble gas ion of 300–3000 eV in energy and a surface atom or ion (Fig. 13-3). A fraction of the bombarding ions leave the surface after only a single binary elastic collision with surface atoms. Through conservation of momentum, an ion scattered at a particular angle retains a specific energy dependent only upon the mass of the surface atom and the energy of the primary beam ion. By scanning the energy of the scattered ion, the ion scattering spectrum is obtained. Knowing the mass, M_0 , and the energy, E_0 , of the primary ion beam, and the energy, E_i , of the particular ion scattered at 90° , the mass of the surface atom, M_i , is determined by the expression

$$\frac{E_i}{E_0} = \frac{M_i - M_0}{M_i + M_0} \quad (13-1)$$

Mapping

sputtering, scribing, prevent attainment using argon ion sput- taking the system. A e adsorption rate of

thick for convenient an surface is to scribe d be about as wide

is ion beam for sput- tion provided in the edment of the speci- men surface while or AES) or with an be much larger than is in the center of of the crater, where

Primary ions that penetrate past the top monolayer of exposed surface atoms do not retain the energy necessary to contribute a signal indicative of the elements present. Thus, the scattered signal is derived entirely from the top exposed layer of atoms on the specimen surface. ISS is sensitive to all elements with atomic number greater than that of the bombarding noble gas ion. The limit of detection is approximately 10^{-4} monolayer; the overall sensitivity is about 1% of the monolayer for most elements.

ISS has limited spatial capabilities; spatial resolution is about 100 μm . For elements of high atomic weight, sputtering with argon ions in place of helium ions improves the response. ISS uses several different noble gas ion species to maximize the element coverage

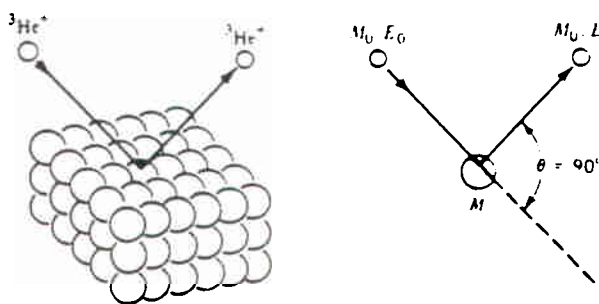


FIGURE 13-3 Elastic collision of noble gas ion and surface atom.

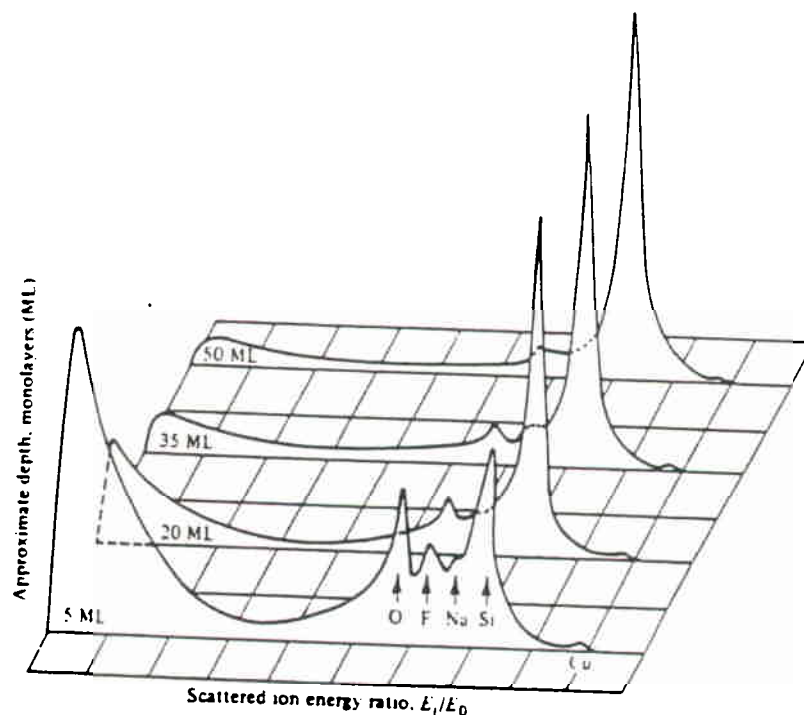


FIGURE 13-4 Depth profiling with ISS; analysis of a silicon wafer from 5 to 50 monolayers.

and mass resolution, since the scattering process is blind to masses below the probe ion's mass and the ability to resolve atoms of similar mass degrades as the difference between the probe ion and target masses increases.

Each particular element of mass M_i will cause scattering of the noble gas ion beam at a unique energy. For example, bombardment with $^3\text{He}^+$ with an incident energy of E_0 , the calculated energy after 90° scattering is $0.684(E_i/E_0)$ from ^{16}O and $0.714(E_i/E_0)$ from ^{18}O . The intensity of a given scattering peak is proportional to the number of scattered ions, and thus is directly related to the amount of material present on the surface.

The probe ion beam can be used in a dual manner to both analyze and to clean the surface controllably. By successive recording of scattering spectra, using controlled beam current densities, a depth-profile composition analysis can be performed, as shown in Fig. 13-4. For $^3\text{He}^+$, the rate of removal generally ranges from 3 to 50 monolayers/hr, thus enabling a single monolayer to be carefully examined or quickly removed. When surface cleaning at a higher rate is desired, a more massive noble gas ion is used, generally argon. In this case, the removal rates are increased by approximately a factor of 10.

ISS is one technique that is sensitive to different isotopic masses. The technique finds use in studying catalytic reaction mechanisms, self-diffusion processes, adsorption-desorption phenomena, the interaction of air pollutants with solid surfaces, or any other reaction involving an exchange of the same atomic species.

to

me

de

me

(3)

ml

pr

me

tor

lim

tra

suc

cor

me

the

dia

be

FIG
(CM)

to, 357

Ion Scattering Spectrometer

The principal components of the ion scattering spectrometer are (Fig. 13-5): (1) a monoenergetic ion gun with excellent focusing properties and controllable current densities that generates the primary ion beam; (2) a high-resolution energy analyzer for measurement of the scattering ion energies which also defines a narrow scattering angle; (3) an ion detector that detects and amplifies the scattered ion signal; (4) a rotatable multiple sample holder that carefully defines the correct sample angle with respect to the primary ion beam and analyzer; and (5) an ion gun drive, controls, and associated instrumentation. In addition there is needed an ultra-high vacuum system with pressure monitoring equipment; a residual vacuum of 10^{-9} torr is obtained with ion and titanium sublimation pumping. Sample charging of insulating surfaces is alleviated with a charge neutralization flood gun.

Ion Source An electron impact ionization source provides a beam of noble gas ions, such as $^3\text{He}^+$, $^4\text{He}^+$, $^{20}\text{Ne}^+$, or $^{40}\text{Ar}^+$, with a low initial kinetic energy spread. The ion source consists of a cylindrical grid with an external filament. Ions formed by electron bombardment of the noble gas inside the grid are extracted axially from one end and focused on the target by an electrostatic aperture lens system. The ion gun produces a nominal 1-mm diameter ion beam throughout an operating range of 300–3000 eV. Beam diameter can be decreased in steps to a minimum of $100\ \mu\text{m}$. Such convenient beam selection permits

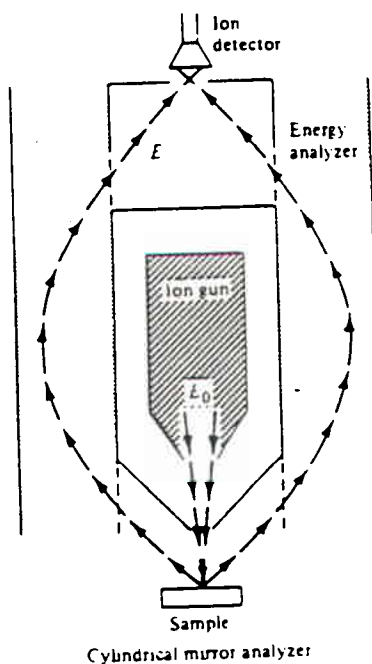


FIGURE 13-5 ISS optical system; ion gun is coaxial with cylindrical mirror analyzer (CMA).

the rapid transition from localized surface analysis with the small beam, to a large area, higher sensitivity analysis where spatial resolution is not critical. By focusing adjustments current densities from 1 to 50 $\mu\text{A}/\text{cm}^2$ are obtained.

Energy Analyzer The ion gun, which is used to form and direct the primary ion beam, normal to the specimen surface, is located coaxially within a cylindrical mirror (energy) analyzer (CMA). The normal incident beam eliminates shadowing caused by surface topography and permits analysis of fine powders without resorting to the use of adhesives to hold them in place.

The CMA accepts those electrons which are emitted within a few degrees of 42.3° ; the acceptance solid angle of this device is about 10% of the total 2π solid angle. The principle of the CMA is based on the electrostatic focusing properties of two coaxial cylinders. With the specimen placed on axis, electrons are allowed to pass into the analyzer through an annular aperture cut in the inner cylinder. A deflecting potential is applied to the outer cylinder, which focuses electrons of a particular energy back onto the axis after they have passed through another annular aperture at exit. As no retardation is involved and only electrons in a very narrow range of energy (about 0.5% of the energy) are passed at any one deflecting voltage, the signal-to-noise characteristics are good. Spectral scan rates of 0.1 sec or faster are possible across the entire energy spectrum. This permits real-time oscilloscopic monitoring and signal averaging of spectral data.

Detector Ion detection is accomplished by use of a channel electron multiplier mounted directly behind the exit slit of the analyzer. The detector is enclosed in an electrostatic shield, electrically common with the analyzer. The detector is operated in a pulse counting mode. Its pulse output is shaped, amplified, and counted.

13.2 SECONDARY ION MASS SPECTROMETRY (SIMS)

In SIMS an energetic primary ion strikes the surface and releases secondary ions. If atomic, these secondary ions are analyzed and detected as such, while molecular ions can dissociate to give positive and negative ion mass spectra for the molecules present in the surface. The SIMS spectrum therefore consists of both those secondary ions which are stable to such dissociation and the ionic fragments of those that are not. SIMS spectra also incorporate features caused by ion-neutral association reactions occurring in the sheath, the region of relatively high pressure just above the surface.

SIMS is a rapid, easily used technique that not only affords qualitative identification of all surface elements (including hydrogen), but also permits identification of isotopes and the structural elucidation of molecular compounds present on a surface and permits very high detection sensitivity (parts per million levels) with a minimum of sample volume (0.2–0.5 nm depth). In addition to depth composition information of about two atomic monolayers, SIMS can also obtain spatially resolved surface information, such as absorbed ion images, elemental line scans, and images of surface constituents. It is capable of unit

mass resolution from hydrogen to its mass limit of 300 daltons. The positive SIMS spectra are extremely sensitive to elements on the left side of the periodic table while the negative SIMS spectra favor the right side. Signal-to-background ratios with SIMS spectra are improved, as compared with ISS, because of the inherent advantages that come with the state-of-the-art quadrupole mass spectrometer. Molecular SIMS shows the characteristic structural specificity of mass spectrometry which extends to isomer and isotopic distinction. Deleterious effects of the sampling ion beam are smaller for organic, as opposed to metallic surfaces, hence higher primary ion currents can be used without causing surface damage.

Given the existence of strong, well-defined bonds between specific atoms in organic compounds, the final bonding pattern revealed in the ionic compositions making up the SIMS spectrum can be related to the surface bonding pattern. The interpretation of SIMS spectra of organic compounds is facilitated by the large body of data available on the dissociations of gas phase organic ions. SIMS spectra incorporate features due to low-energy ion-molecule reactions and to unimolecular dissociations which parallel those observed in other forms of mass spectrometry. While parent ions such as $(M + Ag^+)$ and $(M - H)^+$ are not yet familiar ionic species, the dissociation reactions that they and other secondary ions undergo can be inferred from other forms of mass spectrometry.

While SIMS has been applied mainly to metals and semiconductors, it also has been used for analysis of glass, rare earth compounds, and minerals. One trend is the micro-area analysis by microprobe SIMS. Contributions are being made to important subjects such as analysis of precipitates, grain boundary segregations, and welded bonds, and to some serious problems such as temper brittleness, hot workability, hydrogen embrittlement, and hydrogen-induced cracking.

Ion yields in SIMS are very dependent on and sensitive to the chemical environment in which the ions are formed. The use of oxygen as a bombarding species gives significantly enhanced positive ion yields for electropositive elements in comparison to the yields obtained by using a nonreactive bombarding species such as $^{40}Ar^+$. If Ar^+ is used, positive ion yields can be enhanced by increasing the oxygen pressure in the vicinity of the sample surface.

The interactions of the sample and the primary ion beam are very complex. The matrix effects are extreme, causing variations of up to several orders of magnitude in measured elemental percentages. Generally the secondary ion yield is erratic until a reactive layer forms on the sample and a steady state is reached. The ion yield is then relatively constant, and quantitative analysis can be attempted. In any case, quantitative analysis of the first few monolayers of the sample is especially difficult.

SIMS Instrumentation

Instrumentation for SIMS ranges from simple plasma discharge source/quadrupole mass analyzers to sophisticated ion microprobe mass analyzers (IMMA) and ion micro-analyzers. Whatever the level of sophistication, all instruments employ a source of primary ions, a mass analyzer, and a sensitive secondary ion detector, enclosed in a high vacuum or an ultra-high vacuum chamber. Since the ion beam used in SIMS fulfills the

excitation as well as sputtering requirements of the technique, the ion source is a key part of the instrument and determines many of the instrumental capabilities.

Since the ISS technique also produces sputtered ions from the surface, it is convenient to simultaneously conduct SIMS. In the combined ISS/SIMS system, the incident beam of monoenergetic noble gas ions is directed vertically onto a properly positioned sample. The entrance aperture for the CMA is shown in Fig. 13-5. In the third orthogonal direction from the sample is the quadrupole mass analyzer whose output is the SIMS signal. A prefilter ion lens rejects the neutrals and high-energy ions. Generally, the energy range of the scattered ions is quite different from the energy range of the sputtered ions. This is beneficial for maximal signal-to-noise ratio in both techniques. The sputtered ions have low energies and interfere little with the scattered ion signal in ISS. Because of their low energy, however, the sputtered ions can be easily analyzed in a quadrupole mass analyzer (Chapter 19). The ability of the ISS/SIMS system to generate large amounts of useful information rapidly requires the use of data processing and storage to realize optimum analytical capabilities. These functions are provided through three separate units: a digital multiplexer, a data processor, and a tape drive data storage unit.

Ion Microprobe Mass Analyzer (IMMA) The IMMA type of instrument (Fig. 13-6) uses a microfocused primary ion beam from a duoplasmatron source to provide lateral microanalysis with high spatial resolution ($2\text{--}10\ \mu\text{m}$) as well as surface analysis and in-depth profiling. The impinging ion beam is generated in a duoplasmatron source which is essentially a low-voltage, low-pressure, hot-cathode arc that is capable of producing either positively or negatively charged ions. This source employs a plasma with both electrostatic and magnetic constriction (hence the term *duo*) to produce a high brightness source

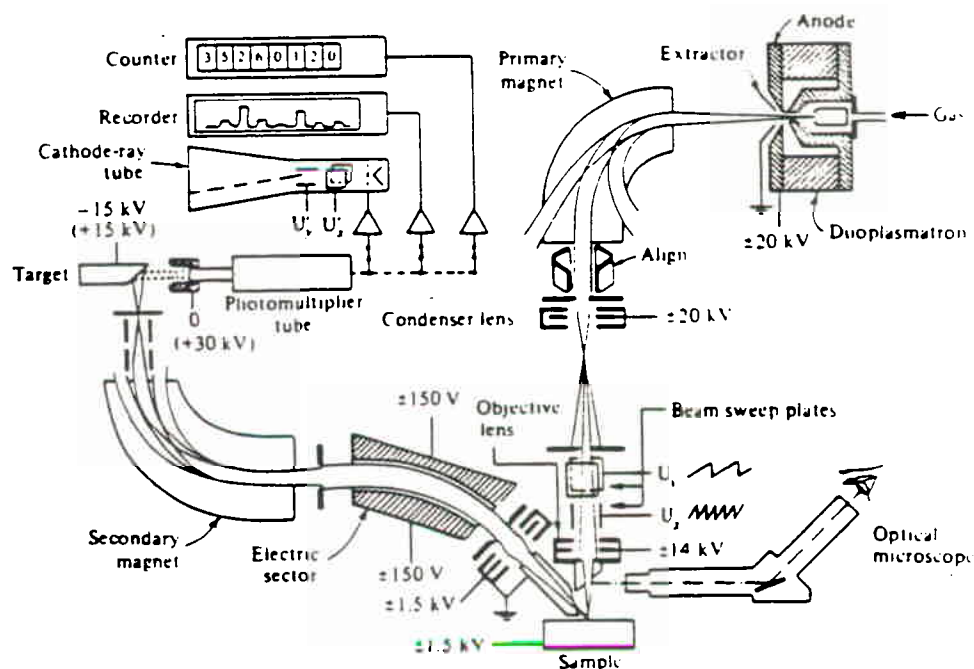
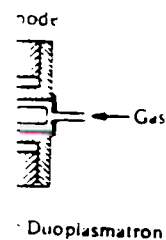


FIGURE 13-6 Schematic diagram of an ion microprobe mass analyzer. (Courtesy of Applied Research Laboratories.)

source is a key part

, it is convenient
the incident beam
positioned sample.
third orthogonal
it is the SIMS sig-
nally, the energy
the sputtered ions.
The sputtered
ISS. Because of
quadrupole mass
large amounts of
to realize opti-
separate units:

ment (Fig. 13-6)
provide lateral
analysis and in-
source which is
producing either
both electro-
brightness source



(Courtesy of

of inert or reactive gas ions (usually either O^+ , F^+ , or Ar^+). Ions are extracted from the source through a hole in the anode and accelerated to energies ranging from 5 to 25 keV. Two electrostatic lenses then provide demagnification of the duoplasmatron source image to produce an ion beam diameter of 2–10 μm . The primary beam spot is held stationary for local analysis or rastered about the sample surface for secondary ion imaging or for producing a flat-bottomed crater for accurate depth profiling.

The duoplasmatron produces a variety of ionized species and, in some cases, ionized molecular fragments. Since it is desirable to have only one type of ion interact with the sample, the primary beam is passed through a mass analyzer placed at the entrance to the electrostatic lens column. The magnetic field is adjusted so that only the desired ion is deflected into the lenses. The composition of the primary beam can be checked by using a sample surface as an electrostatic mirror, thereby deflecting a fraction of the primary beam into the mass spectrometer. In IMMA the magnetic field is the wedge-type with plane but inclined pole pieces. In the less sophisticated ion microanalyzer, the source mass analyzer is omitted.

Sorting out the sputtered secondary sample ions by mass charge ratio is accomplished in the IMMA system by a two-stage mass spectrometer. The first-stage electrostatic sector sorts the ions on the basis of velocity and brings most of them to a similar speed. Next, the second-stage magnetic sector sorts the ions on the basis of mass charge ratio. Only those ions having a discrete selected ratio are passed through the exit slit to the detector. By varying the magnetic field strength, the entire mass range from 1 to 300 daltons can be scanned in 30 sec. An electrostatic lens increases the angular aperture of the detector.

13.3 AUGER EMISSION SPECTROSCOPY (AES)

AES measures electrons emitted from a surface, induced by electron bombardment. The first step is ionization of an inner atomic level by a primary electron. Once the atom is ionized it must relax by emitting either a photon, as discussed in Chapter 9, or an electron—the nonradiative Auger process. In most instances nature chooses the Auger process. For example, a *KLL* Auger transition means that the *K* level electron undergoes the initial ionization. An *L* level electron moves in to fill the *K* level vacancy and, at the same time, gives up the energy of that transition (*L* to *K*) to another *L* level electron which then becomes the ejected Auger electron. Other Auger electrons originate from *LMN* and *MNN* transitions. At this point the atom is doubly ionized. The energy of the ejected electron is a function only of the atomic energy levels involved in the Auger transition, and is thus characteristic of the atom from which it came. A threshold energy, related to the transition energy, exists and a primary energy of 5–6 times the Auger energy maximizes the sensitivity to that particular transition. All elements except hydrogen and helium, produce Auger peaks. Most elements have more than one intense Auger peak, so that a recording of the spectrum of energies of Auger electrons released from any surface, compared with the known spectra of pure elements, enables a chemical analysis to be made.

Because the X-ray and Auger emission processes are competitive, the relative sensitivities of these two techniques are complementary when considering the relative abun-

dance of X rays and Auger electrons after ionization of a particular level. In the light elements ($Z < 30$), the Auger process dominates, which makes AES relatively more sensitive. For heavier elements the electron microprobe (Chapter 9) becomes more sensitive for transitions following ionization of inner shells. The sensitivity of AES is maintained, however, by utilizing Auger transitions between outer shells, for example *MNN*, where the Auger process dominates.

Although the penetration of the primary electron beam is several atomic layers, the Auger electrons are on the average of much lower energies. Electrons of such low energy must originate very close to the surface if they are to escape without being lost by inelastic scattering before reaching the surface. Typically, Auger electrons come from the first few atomic layers; the sampling depth is about 2.0 nm.

The sensitivity of the Auger technique is determined by the probability of the Auger transitions involved, the incident beam current and energy, and by the collection efficiency of the energy analyzer. With a high-sensitivity CMA, the detection limit for the elements varies between 0.1 and 1 atomic percent (or 10^{-3} of a monolayer). Because the electron beam can be focused to a small diameter (50.0 nm), it is possible to do spatial resolution on a sample. Operated in this mode, AES is usually referred to as the Auger microprobe. AES is traditionally run with high-intensity electron guns and low-resolution analyzers, resulting in fast analysis speed. Unfortunately, this limits one to primarily elemental information with little information on chemical bonding, such as one clearly obtains in the chemical shifts of ESCA or in the molecular fragments found in SIMS. For example, hydrocarbon compounds appear in AES only as a C peak, since H is not observed.

Figure 13-7 shows the Auger spectra of Ag, Cd, In, and Sb, in these cases the *MNN* transitions. The spectra are very similar with the only major difference being the shifts in energy from one element to the next. These shifts are of the order of 25 eV and, since the peak positions can be measured to an accuracy of ± 1 eV, there is no ambiguity in identification of adjacent elements in the periodic chart. Auger spectra of all the elements lie between 50 and 1000 eV. The *KLL* transitions correspond quite nicely with tabulated X-ray energies. There are, however, some minor differences due to the energy Auger electrons must lose in escaping from the sample. The Auger lines are relatively broad because of the double uncertainty of the origins within a band of both the downward and upward electrons involved in the Auger process. Lines due to *LMM* transitions also tend to correlate with X-ray energies, but some lines are beginning to appear which the selection rules for photon emission forbid. The selection rules must be relaxed for the radiationless Auger process. As the atomic number increases, the Auger spectra become more complex and overlapping may occur.

The strength of AES lies in its ability to give both a qualitative and quantitative non-destructive analysis of the elements present in the immediate atomic layers from a very small area of a solid surface. When combined with a controlled removal of surface layers by ion sputtering, AES provides the means to solve some very important problems. To provide ion sputtering for surface cleaning and/or depth profiling, the sample chamber is backfilled with argon and an electron impact ion source used, as in ISS.

FIGURE 13-7
Auger spectra

AES

1
carr
(Fig
spu
ava
wit

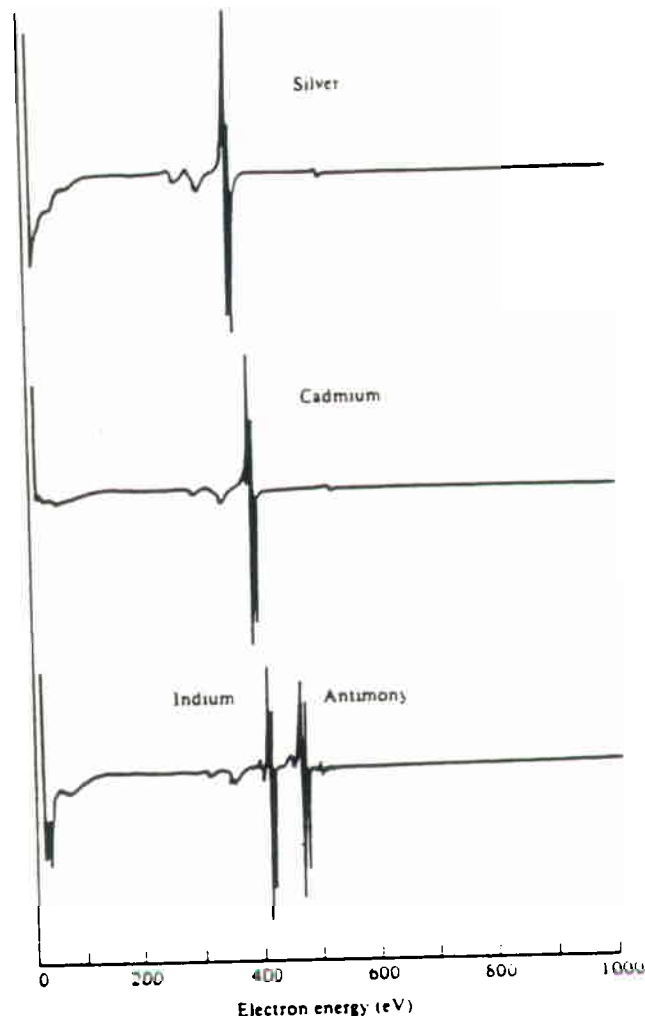


FIGURE 13-7 Auger spectra (differential form) from silver, cadmium, indium, and antimony; all are *MNN* transitions.

AES Instrumentation

The Auger spectrometer consists of an ultra-high vacuum chamber console, a sample carousel and manipulator unit, and a combination electron gun/energy analyzer unit (Fig. 13-8). Auxiliary equipment often includes a grazing incidence electron gun and a sputter ion gun for cleaning surfaces and for profiling studies. Auger spectrometers are available as large-beam ($\sim 25 \mu\text{m}$) depth-profiling instruments or as Auger microprobes with beam diameters of $5 \mu\text{m}$. If an instrument is to be used as a high-sensitivity depth

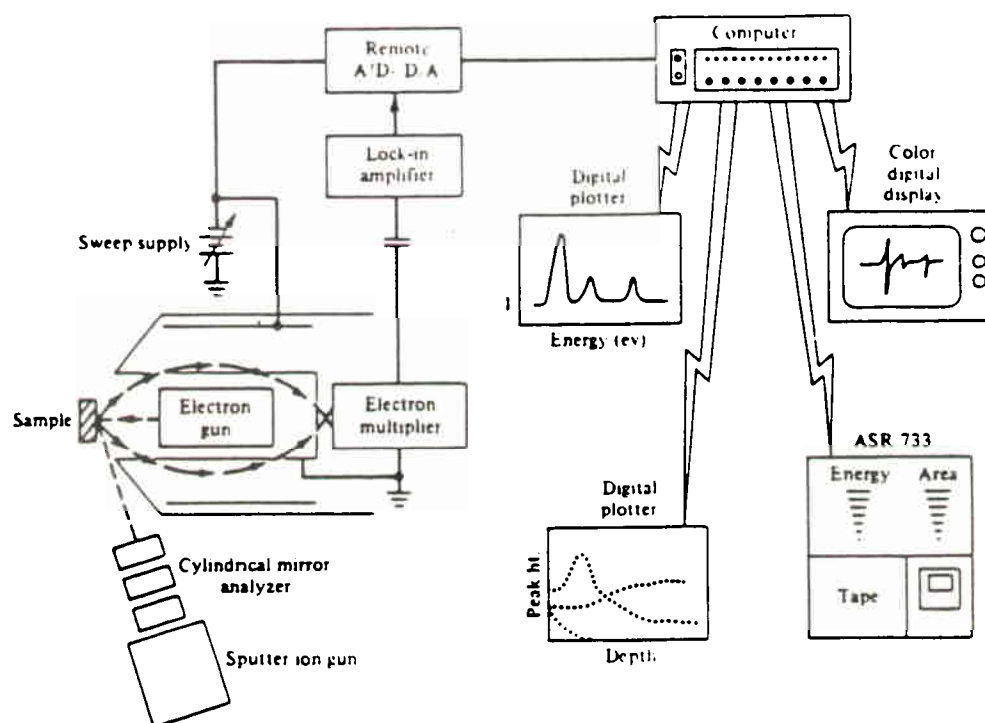


FIGURE 13-8 Schematic diagram of an Auger spectrometer with computer control.

profiler and also as a high lateral resolution microprobe, two electron guns may be required to realize optimum use of each operating mode.

The energy distribution of electrons emitted from the target, $N(E)$, is evaluated by scanning the negative voltage applied to the outer cylinder of the CMA. Thus, as the voltage applied to the outer cylinder is scanned, the secondary electron distribution is generated by the current output of the analyzer. Because the Auger peaks are superimposed on a rather large continuous background of secondary electrons, it has become popular to differentiate electronically the $N(E)$ function. This is accomplished by applying a small ac voltage on the dc energy selecting voltage and synchronously detecting the in-phase component of the output current of the electron multiplier with a lock-in amplifier. Unfortunately, the use of the lock-in amplifier in data acquisition places significant limits on sensitivity and quantification of the data. The limitations can be substantially reduced through the use of digital techniques. The digital storage of signal-averaged data with a high dynamic range makes it possible to use digital filters to remove high-frequency noise components from the signal. Signal averaging using multiple passes over a given energy window can be used to ensure that the statistical noise and the Auger peaks of interest present different spatial frequencies. This separation in frequency allows the postacquisition processing of these data to remove the high-frequency noise. In this way, one can substantially improve the elemental sensitivity without serious loss of energy resolution. Consequently, one now has a means for preserving the chemical shift information, while

improves
choice
element

Quant

The
analysis
the co
because
cases
also m
on pe
In
limits
under
ferent
permi
and a

Scan

Th
ysis c
an An
and a
or an
or an
Ti
An x
will g
Ti
large
a sm
as th
Elem
A
ters
200
even
wher
M
dept
data

improving sensitivity for elements present in low concentration. In effect, this allows the choice between energy resolution (that is, oxidation state information as in ESCA) and elemental sensitivity to be made well after the data are acquired.

Quantitative Analysis in AES

The difficulties in the quantification of Auger data are illustrated in depth-profiling analysis. In this operation the change in peak shape of the differentiated spectra distorts the conventional peak-height estimates of concentration. Changes in peak shape can occur because of changes in oxidation state of the emitting atom. This is particularly severe in cases where bonding orbitals are involved in the Auger transitions. Peak-shape changes also may be induced by matrix effects, since the energy loss mechanisms and their effect on peak shape may be dominated by matrix elemental composition.

In order to provide accurate quantitative information within the normal quantitative limits of AES, it is necessary to use the total Auger current. This is expressed by the area under the curve for the peak of interest, with background subtracted. By using undifferentiated data and integrating the total number of Auger electrons in the peak, one is permitted a choice of the limits of integration. Now, chemical shifts may be observed, and a depth profile is realized without the artifacts.

Scanning Auger Microprobe (SAM)

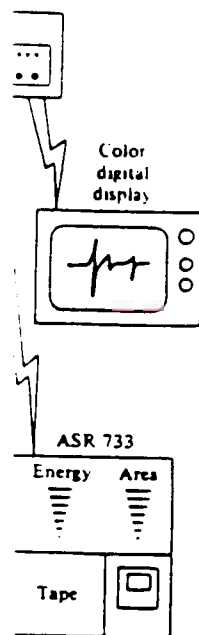
The SAM employs a finely focused, scanning electron beam as the probe for AES analysis of a given surface. For a surface area, the SAM will provide an electron micrograph, an Auger image of selected elements on a CRT display for observation or photographing, and a depth-composition profile. First, the CRT image is used to determine specific points or an area of interest on the sample. From the micrograph obtained, points of interest or an area up to 200 μm can be chosen for compositional analysis.

The image mode is useful because position of elements are delineated in a few minutes. An x-y recording of a line scan across a selected region of the image for a given element will give a relative quantitative measure of its concentration.

The thin film analyzer mode of the SAM simultaneously sputter-etches a relatively large surface area (several millimeters in diameter) and multiplexes the Auger signals from a smaller area about 15 μm in diameter. Up to six selected Auger peaks can be recorded as the surface is etched. Depth resolution is about 10% of the total etched thickness. Elements are detected when present in quantities down to 0.1% of monolayer.

At best, the spatial resolving power of SAM is 500 nm with tungsten thermionic emitters as the electron source. The use of LaB_6 emitters extends the resolving power to 100–200 nm because of their high electron optical brightness. Field emitters, which provide even higher brightness, are expected to allow one to analyze smaller areas in less time when they come into use.

Many surface composition problems involve compositional inhomogeneity, both in-depth and across a material surface. Scanning Auger microscopy often provides a more detailed characterization of material that exhibits inhomogeneous composition. SAM



computer control.

guns may be re-

is evaluated by
us, as the voltage
ion is generated
reimposed on a
popular to dif-
fusing a small ac
ie in-phase com-
nplifier. Unfor-
ficant limits on
ntially reduced
ged data with a
frequency noise
a given energy
eaks of interest
the postacquisi-
s way, one can
ergy resolution.
ormation, while

offers high spatial resolution, in the form of SEM-type imaging combined with elemental mapping capabilities. For example, graphite present in spherical nodules indicates that the specimen of cast iron is ductile cast iron. Examination of the carbon Auger images shows carbon to be present in both the graphite nodules and, at lower concentration, in regions between nodules. Carbon is not evident in the circular regions around nodules. The iron Auger image shows iron to be present everywhere in the specimen surface except in the graphite regions.

Spatially resolved SIMS is especially useful when combined with SAM, as suggested by the study of an automotive ignition contact. A high-resolution absorbed current SAM image of the contact obtained first showed detailed surface topography. An absorbed ion current image was then obtained and compared with the SAM image to identify specific areas of interest for further study. High-sensitivity SIMS point analysis was performed at the center and the outer edge of the contact. The resulting spectra showed higher concentrations of calcium and iron in the center region of the contact, as indicated by the large increase in the Ca^+/K^+ and Fe^+/Ni^+ ratios, compared to the spectrum from the side of the contact.

13.4 ELECTRON SPECTROSCOPY FOR CHEMICAL ANALYSIS (ESCA)

ESCA is concerned with the measurement of core-electron binding energies. A molecule or atom is bombarded with a source of high-energy X rays which cause the emission from sample atoms of inner-shell electrons. All electrons whose binding energies are less than the energy of the exciting X rays are ejected. The kinetic energies, E_k , of these photoelectrons are then measured by an energy analyzer. The core-electron binding energies, E_b , relative to the Fermi level* can then be computed via the relationship

$$E_b = h\nu - E_k - \phi \quad (13-2)$$

where $h\nu$ is the energy of the exciting radiation and ϕ is the spectrometer work function, a constant for a given analyzer. Binding energies unambiguously define a specific atom. AES can be compared to ESCA because both originate from similar fundamental processes. In ESCA the ionizing source is an X-ray photon that ejects an inner-core electron, whereas in AES the electron ejection is caused by an impinging electron. The photoelectron escape depths are the same as those for Auger electrons of the same kinetic energy. The energy of the ejected electron (Auger electron or E_k) is thus characteristic of the atom involved and its chemical environment.

Although the X-ray photon may penetrate and excite photoelectrons to a depth of several hundred nanometers, only the photoelectrons from the outermost layers have any

*The quantum mechanical (chemical) zero of energy, called the vacuum level for gaseous systems, is the zero of energy determined by following the potential energy interaction of an electron as it is removed to infinity with respect to its parent atom. When the system being examined is a solid, the quantum-mechanical zero in energy is the Fermi level. The Fermi level differs from the vacuum level by the amount of energy that is needed to remove the electron, already outside its chemical environment, from its physical environment, that is, the surface. This extra energy for a material is proportional to the work function.

chance to escape from the material environment and to be eventually measured. Most ESCA measurements of solids generate useful information from only the outer 2.0 nm of the surface layer.

The required sample size is a microgram or less. The sampling area is approximately 1 cm^2 . Applicability to the second row elements, including carbon, nitrogen, and oxygen, makes ESCA an important structural tool for organic materials. The detection limit depends on the particular element being measured, but will range from 1% of a monolayer for light elements to 0.1% of a monolayer for heavy elements.

To determine the absolute binding energy, the work function of the sample and of the spectrometer must be known. Unfortunately, the work function is not independent of the physical state of the material; neither is it easy to measure or calculate. The problem can be circumvented for many materials by employing a physical trick. If the material being examined is a conductor, it usually is possible to couple the conduction bands of the material with that for the spectrometer, which presumably is also a good conductor. The coupling is such that the Fermi levels of the material and the spectrometer merge. The value of ϕ may also be calculated relative to a reference element, such as carbon (1s) or gold spectral features.

Frequently, only a relative binding energy (chemical shift) is desired in chemical studies. Here it is sufficient that ϕ be constant. For example, the chemical shift of a metal oxide relative to the metal may be calculated from the measured kinetic energies:

$$\Delta E_{\text{oxide}} = E_{k(\text{metal})} - E_{k(\text{oxide})} \quad (13-3)$$

It is ΔE_{oxide} , the chemical shift, which gives chemical structure information.

Chemical Shift

The utility of ESCA for the chemist is the result of chemical shifts that are observed in electron binding energies. The binding energies of core electrons are affected by the valence electrons and therefore by the chemical environment of the atom. When the atomic arrangement surrounding the atom ejecting a photoelectron is changed, it alters the local (quantum) charge environment at that atomic site. This change, in turn, reflects itself as a variation in the binding energy of *all* the electrons of that atom. Thus, not only the valence electrons, but also the binding energies of the core electrons experience a characteristic shift. Such a shift is inherent to the chemical species producing the results and thus provides the capability of chemical analysis. In a simple sense, the shifts of the photoelectron lines in an ESCA spectrum reflect the increase in binding energy as the oxidation state of the atom becomes more positive. In general, any parameter, such as oxidation state, ligand electronegativity, or coordination, that affects the electron density about the atom is expected to result in a chemical shift in electron binding energy.

A major portion of the strength of ESCA as an analytical tool lies in the fact that chemical shifts can be observed for every element in the periodic chart except for hydrogen and helium. Magnitudes of chemical shifts will vary from element to element, and the sensitivity for a particular element will vary with the photoelectron cross section. In general, the ESCA chemical shifts lie in the range 0–1500 eV. For instance, the position

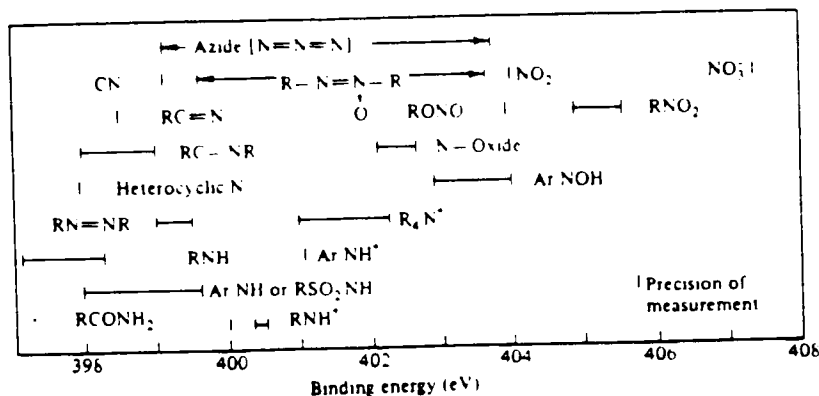


FIGURE 13-9 Correlation chart for nitrogen (1s) electron binding energies and organic functional groups.

of the nitrogen 1s peak at a binding energy of 398 eV correlates very well with nitrogen being in a formal oxidation state of -1 . In order to make this assignment one must refer to a catalog of reference nitrogen spectra or to correlation charts, such as Fig. 13-9. One should be cautious about making structural assignments on the basis of small ESCA binding energy shifts since factors such as crystal potential energy differences and sample charging can cause apparent shifts of the order of magnitude of the observed chemical shifts.

In general, photoelectron peaks are narrower than the corresponding X-ray emission lines, and in most cases, vary from 1 to 3 eV (FWHM). Since the chemical shifts for a given element are of the order of 10 eV, ESCA is not a high-resolution method. The FWHM resolution of about 1.0 eV makes it possible to resolve electron energies that differ by about 0.5–1.0 eV, and thus to measure chemical shifts which are of interest to most chemists. For example, Fig. 13-10 shows the partial ESCA spectrum of Cu_2O , CuO , and metallic copper. One could clearly distinguish between metallic copper and CuO , but it would be difficult to decide between metallic copper and Cu_2O . However, by also observ-

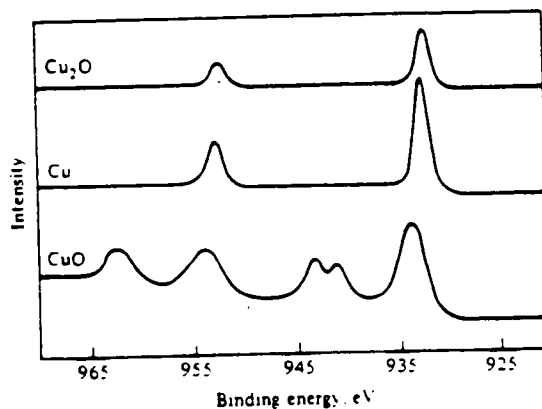


FIGURE 13-10 ESCA spectra of Cu_2O , CuO , and metallic copper.

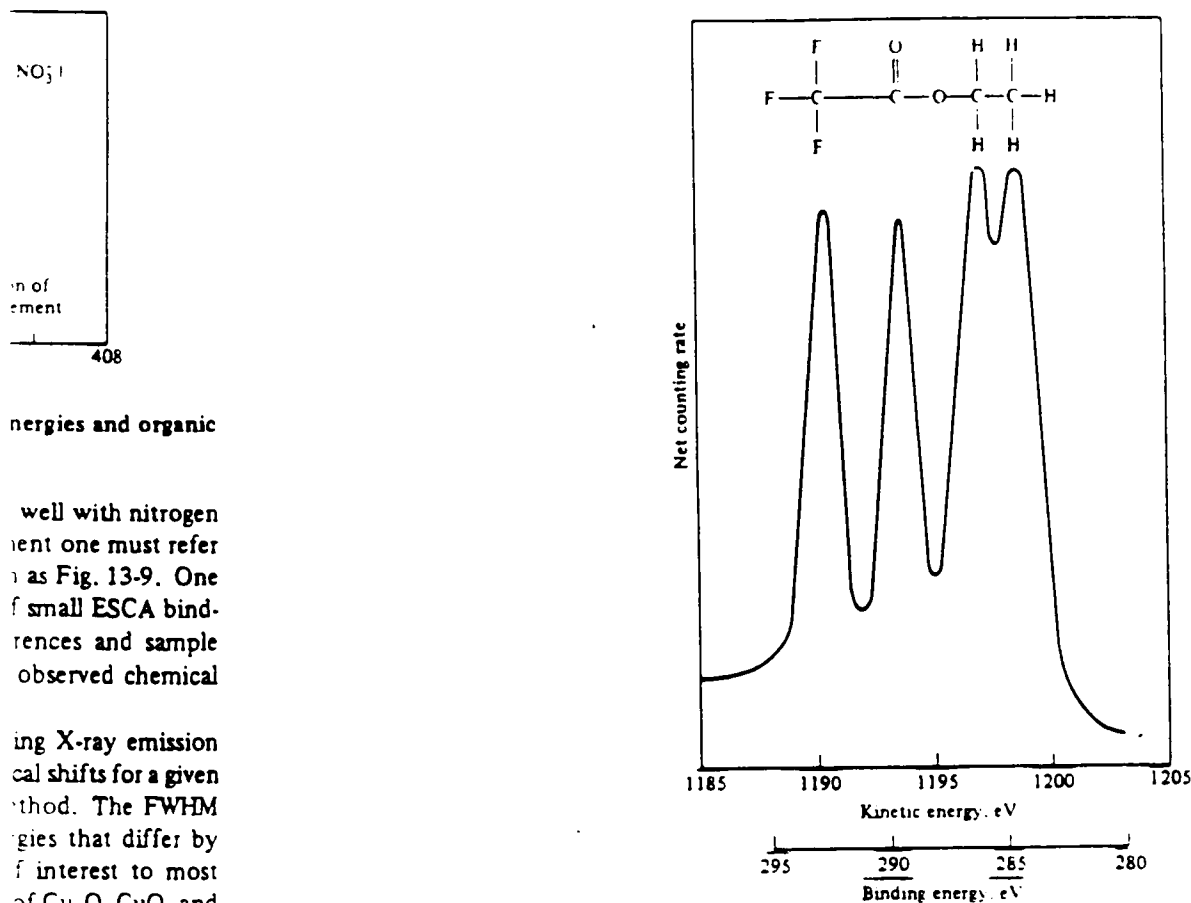


FIGURE 13-11 ESCA spectrum of ethyltrifluoroacetate.

ing the oxygen 1s spectrum (530.8 eV for Cu_2O and 530.1 eV for CuO), one can easily distinguish between metallic copper and its two oxidation states. The classic example of chemical shifts is the carbon 1s ESCA spectrum of ethyltrifluoroacetate shown in Fig. 13-11. Each carbon atom is located in a different chemical environment and the ESCA spectrum contains four distinct photoelectron lines. The trifluorocarbon yields the photoelectron line at highest binding energy since the fluorine atoms withdraw electron density from the carbon atom most efficiently. In this example, the relative positions of the photoelectron lines reflect the relative electronegativity of the various substituents; the respective carbon photoelectron lines actually appear above their peaks in the spectrum.

ESCA Instrumentation

Instrumentation for ESCA, shown in Fig. 13-12, involves a radiation source of sufficient energy to eject an electron from the sample. There must also be a device that collects the emitted electrons, counts them, and carefully measures their kinetic energy. A

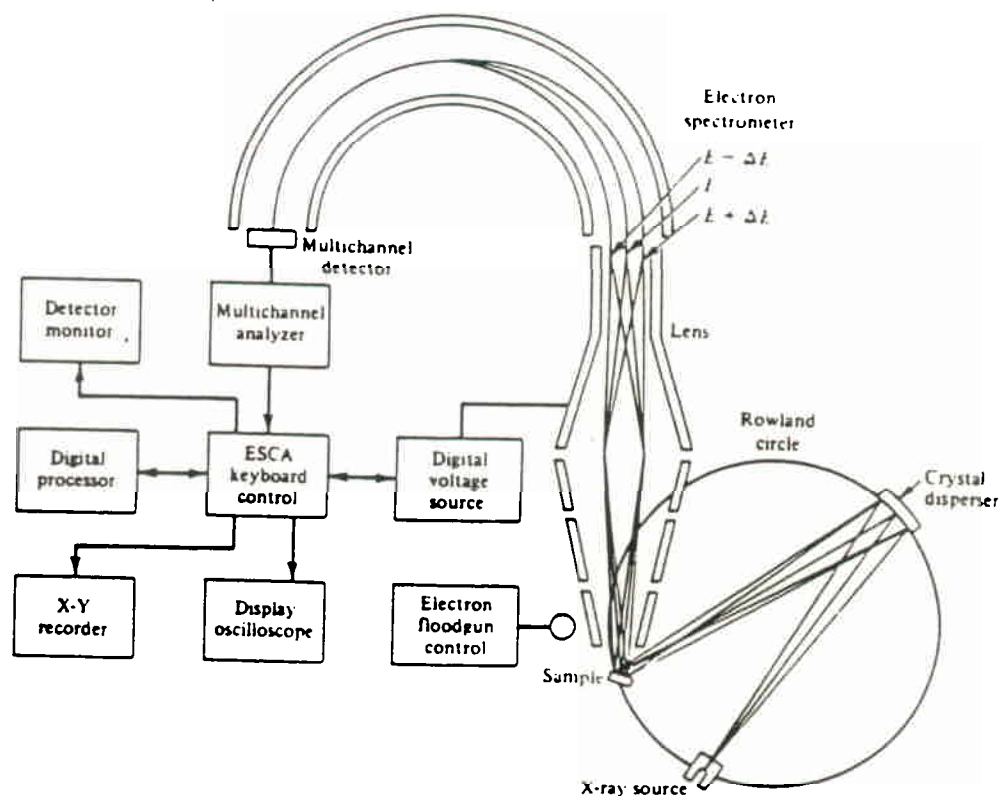


FIGURE 13-12 Schematic of an ESCA spectrometer using crystal dispersion to achieve X-ray monochromatization and a digital processor. Commercial version is the Hewlett-Packard model 5950B.

storage and display unit is usually included. Since it is necessary to ensure that the mean free path of the photoelectrons is large enough to allow them to traverse the distance from the sample to the detector without suffering energy loss, ESCA is a vacuum technique with a maximum operating pressure of about 5×10^{-6} torr.

ESCA spectra can be obtained on solids, liquids, and gases; the physical form of the sample is not important. However, the technique is a vacuum technique; therefore, low vapor pressure solids are most easily run. A solid sample need only be placed on a probe that is appropriately positioned relative to the X-ray beam and the spectrometer slit. Liquids cannot be run as such, but must be condensed onto a cryogenic probe and run in the condensed phase. Alternatively, liquids can be vaporized and run in the gaseous state. To obtain spectra on the gaseous sample, the spectrometer must be equipped with a differential pumping system to prevent the pressure in the analyzer from rising above 10^{-6} torr.

Source Soft X rays, such as $\text{Mg } K\alpha_{1,2}$ and $\text{Al } K\alpha_{1,2}$ with a FWHM of 0.75 and 0.95 eV, respectively, are usually employed for photoelectron excitation. It is important to

have at least two alternate sources in order to distinguish photoelectron peaks from Auger peaks. When a different X-ray source is used, the photoelectron peaks shift in kinetic energy but the kinetic energies of Auger peaks remain constant and appear at the same energy position in the spectrum. A source of small linewidth is advantageous to have if an element exists in several oxidation states in a sample and it is desired to extract the binding energies of each of these oxidation states.

Two types of X-ray systems are used in commercial instruments. In one the sample is illuminated directly by the output of the source. This polychromatic type of source is quite simple and permits the use of different target materials and hence different energies of photoelectron excitation. The other system incorporates an X-ray monochromator to disperse the X radiation and thus provide monochromatic illumination of the sample surface. Spectral interferences and background are thereby reduced but X-ray intensities impinging on the sample surface are much lower.

The monochromatic source shown in Fig. 13-12 places the X-ray anode, a spherically bent crystal disperser, and the sample on a Rowland circle. Only the X radiation from the anode is reflected to the sample by the crystal. The source radiation will be free from the X-ray satellite structure (arising from $K\alpha_{3,4}$ and $K\beta$ lines) that plagues the photoelectron spectra generated with polychromatic beams. Elimination of the broad background bremsstrahlung radiation improves the signal-to-background ratio and sharply reduces X-radiation damage in the sample. For example, radiation-induced changes, such as reduction of Cu(II) to Cu(I), that occur in 20 sec with bremsstrahlung radiation, will only occur after 10 hr with the crystal-reflection method.

ESCA Electron Analyzers The electron analyzers used in ESCA instrumentation employ the double-focusing principle. An electrostatic field sorts the electrons. As the field is varied, electrons of appropriate kinetic energy are focused at the detector. Initially, in the instrument illustrated, the photoelectrons are channeled through a series of four interconnected electrostatic lenses. This method for photoelectron collection is referred to as dispersion compensation, with the four lenses acting as selective apertures. In addition, a retarding voltage is employed to bring the photoelectrons into focus so that the inherent linewidths of the X-ray photon can be removed. In addition, the lenses provide the mechanism for selecting and scanning the particular photoelectron energy of interest.

Detector Both continuous channel and discrete dynode electron multipliers are used to count the electrons. The continuous channel detector counts electrons with high efficiency to very low energies and, compared to discrete dynode multipliers, are more stable to atmospheric and other gases.

Scan and readout systems are either of a continuous or incremental type. In the continuous mode the focusing field is increased continuously as a function of time as the signal from the detector is simultaneously monitored by a rate meter. The focusing field and output from the rate meter are synchronized to allow accurate recording of spectra. In the continuous mode the energy region of interest can be scanned only once. This is somewhat of a handicap since no signal averaging can be performed. Signal averaging becomes necessary when the signal is weak or the quantity of sample is small.



n to achieve
the Hewlett-

at the mean
the distance
vacuum tech-

form of the
erefore, low
d on a probe
rometer slit.
e and run in
aseous state.
d with a dif-
above 10^{-6}

.75 and 0.95
important to

The incremental scanning mode increases the field in a series of small steps, counting the signal during each increment. When the counting rate at each increment is plotted as a function of focusing field, a spectrum is produced. Instrumentation using the incremental scanning mode uses either a multichannel analyzer or a small dedicated computer to accumulate the data. In such systems, signal averaging can be achieved by performing repetitive scans over the energy region of interest. The counting rate in each increment is added to the preceding one. When the system contains a dedicated computer, both control of energy scan and data acquisition are under its control. Usually several energy regions can be scanned sequentially, with the computer storing the data until they are retrieved by the operator.

For display the digital nature of the results makes it convenient to use a point plotter. Spectra of two formats are generated. First step in an analysis is to run a 0–1000 eV survey scan that displays peaks from all major components of the sample. A scan time is automatically chosen by the computer that is optimum for the span and memory channels used. Next, each spectrum interval where peaks appear is examined separately in more detail giving the analytical data needed to identify an element and its relative amount.

Scanning ESCA

ESCA in its earlier years was always thought of as a low spatial resolution technique because the specimen is excited by flooding the surface with X rays. These X rays could not be readily focused. Thus, elemental images could not be generated in a manner analogous to that of SAM where the source of excitation, a scanning electron beam, is focused to a small spot. However, if a focused electron beam is used to bombard a thin foil of aluminum which has a thin specimen mounted on the side opposite the beam a localized source of Al K α X rays is produced in the aluminum foil (Fig. 13-13). This causes a spatially localized source of photoelectrons to be created in the specimen (but also containing satellite structure and bremsstrahlung radiation). The result is an ESCA spectrum

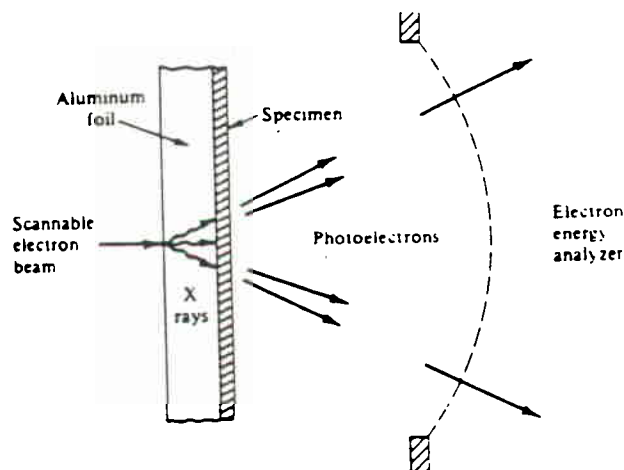


FIGURE 13-13 Schematic arrangement for spatially resolved ESCA.

from an area less than 20 μm in diameter. If a scanning electron beam is employed, two-dimensional photoelectron images can be obtained.

A practical example of the use of surface analysis involved the study of a metallographically polished cast iron specimen. An ESCA survey spectrum indicated the presence of Fe, O, and C as major components of the material. High-resolution spectra of Fe and C showed the presence of both oxidized and reduced iron species and of at least two carbon species. Detailed analysis of the carbon binding energies revealed the presence of a carbide and a species with a binding energy characteristic of graphite. These conclusions are consistent with the fact that cast iron contains precipitated graphite as well as phases rich in iron carbide. The oxidized iron species probably was due to surface oxidation of the specimen.

Quantitative Analysis

The intensity of a photoelectron line is proportional to not only the photoelectric cross section of a particular element, but also to the number of atoms of that particular element that are present in the sample. Analyses of mixtures are often accurate to $\pm 2\%$. An example involves measuring the intensities of photoelectron lines in spectra obtained from mixtures of MoO_2 and MoO_3 at binding energies that correspond to each oxide. No instrumental technique had existed that was capable of performing this analysis. Even though the surface of MoO_2 was significantly contaminated with MoO_3 , a linear calibration curve resulted. Mixtures of PbO-PbO_2 , $\text{Cr}_2\text{O}_3\text{-CrO}_3$, and $\text{As}_2\text{O}_3\text{-As}_2\text{O}_5$ can also be measured quantitatively. Estimates of the total protein content of various grains can be made by measuring the intensities of the nitrogen and sulfur peaks.

BIBLIOGRAPHY

- Barr, T. L., "Applications of ESCA in Industrial Research," *Am. Lab.*, p. 65 (November 1978); p. 40 (December 1978).
- Betteridge, D. and A. D. Baker, "Analytical Potential of Photoelectron Spectroscopy," *Anal. Chem.*, 42, 43A (1970).
- Carlson, T. A., *Photoelectron Auger Spectroscopy*, Plenum, New York, 1975.
- Czanderna, A. W., Ed., *Methods of Surface Analysis*, Elsevier, New York, 1975.
- Davis, L. E., N. C. MacDonald, P. W. Palmberg, G. E. Riach, and R. E. Weber, *Handbook of Auger Electron Spectroscopy*, 2nd ed., Physical Electronics Industries, Eden Prairie, Minn., 1976.
- Day, R. J., S. E. Unger, and R. G. Cooks, "Molecular Secondary Ion Mass Spectrometry," *Anal. Chem.*, 52, 557A (1980).
- Evans, C. A., Jr., "Secondary Ion Mass Analysis," *Anal. Chem.*, 44, 67A (1972).
- Evans, C. A., Jr., "Surface and Thin Film Compositional Analysis: Description and Comparison of Techniques," *Anal. Chem.*, 47, 818A (1975).
- Evans, C. A., Jr., "Surface and Thin Film Analysis: Instrumentation," *Anal. Chem.*, 47, 855A (1975).
- Harris, L. A., "Auger Electron Emission Analysis," *Anal. Chem.*, 40, 24A (1968).

- Heinrich, K. F. J. and D. E. Newbury, Eds., *Secondary Ion Mass Spectrometry*, NBS Special Publ. No. 427, GPO, Washington, D. C., 1975.
- Hercules, D. M., "Electron Spectroscopy," *Anal. Chem.*, **42**, 20A (1970).
- Hercules, D. M., "Challenges in Surface Analysis," *Anal. Chem.*, **50**, 734A (1978).
- Kane, P. F. and G. B. Larrabee, Eds., *Characterization of Solid Surfaces*, Plenum, New York, 1974.
- Karasek, F. W., "Developments in ISS/SIMS," *Research/Development*, p. 26 (January 1978).
- Lee, L. H., Ed., *Characterization of Metal and Polymer Surfaces*, Vol. 1, Academic, New York, 1977.
- Liebl, H., "Ion Microprobe Analyzers: History and Outlook," *Anal. Chem.*, **46**, 22A (1974).
- Lucchesi, C. A. and J. E. Lester, "Electron Spectroscopy Instrumentation," *J. Chem. Educ.*, **50**, A205, A269 (1973).
- Riach, G. E. and R. F. Goff, "Electrons or Ions," *Industrial Research*, p. 84 (June 1974).
- Sparrow, G. R., "Ions Working for You," *Industrial Research*, p. 81 (September 1976).
- Swartz, W. E., Jr., "X-Ray Photoelectron Spectroscopy," *Anal. Chem.*, **45**, 788A (1973).